Phase-Separation Kinetics in the Two-Dimensional Long-Range Ising Model

Fabio Müller,* Henrik Christiansen,†,‡ and Wolfhard Janke‖
Institut für Theoretische Physik, Universität Leipzig, IPF 231101, 04081 Leipzig, Germany

(Received 18 July 2022; accepted 8 November 2022; published 9 December 2022)

Using Monte Carlo computer simulations, we investigate the kinetics of phase separation in the two-dimensional conserved Ising model with power-law decaying long-range interactions, the prototypical model for many long-range interacting systems. A long-standing analytical prediction for the characteristic length is shown to be applicable. In the simulation, we relied on our novel algorithm which provides a massive speedup for long-range interacting systems.

DOI: 10.1103/PhysRevLett.129.240601

Phase separation is relevant not only for many practical applications [1–3] but also from a theoretical point of view [4–6] and is one of the most fundamental processes that leads to pattern formation. It is observed in fields ranging from quantum physics [1,7–9] and biological science [2,10–14] to cosmology [15,16], spanning all relevant length and interaction scales. In many of these fields, the involved forces are inherently long range [17–24]. To understand the underlying processes and the most fundamental scaling laws, we focus here on the kinetics of phase separation in the two-dimensional long-range Ising model (LRIM) with conserved order parameter, which is a prototype model for binary mixtures with long-range interactions. It has the Hamiltonian

$$\mathcal{H} = -\sum_{i<j} J_{i,j} s_i s_j, \qquad J_{i,j} = r_{i,j}^{-(d+\sigma)}, \tag{1}$$

where $s_i = \pm 1$ are spins and $r_{i,j}$ is the distance between s_i and s_j. Here, d is the dimension, and the parameter σ can be used to tune the power-law decay of the couplings $J_{i,j} > 0$, enabling one to investigate systems belonging to different universality classes.

To study the phase-separation kinetics in this model, initially, equally many up and down spins are randomly placed on a square lattice (magnetization $m \equiv 0$), corresponding to an equal volume fraction in a particle picture. Subsequently, the system is quenched below the critical temperature and evolved through local Monte Carlo Kawasaki dynamics [25]. In this type of dynamics, the spins are only allowed to exchange the position with one of their nearest neighbors, keeping the overall order parameter conserved.

Since with long-range interactions all spins interact with each other, *a priori*, one has to take into consideration $\sim N$ interactions at every proposed spin exchange to reach a decision according to the Metropolis criterion. This has hitherto hindered the investigation of large systems which in the presence of long-range interactions need to be even larger than for short-range interacting systems due to stronger finite-size effects. In the past there have been several algorithmic developments to mitigate the problem stemming from the inherent $O(N^2)$ computational complexity. One category comprises Monte Carlo algorithms that circumvent the calculation of the energy differences involved in the updates [26–29] which, however, do not reproduce the desired Metropolis dynamics. Other algorithms directly speed up the evaluation of the energy difference needed for the decision about the attempted updates [30–32] and are thus in principle applicable for the simulation with Metropolis dynamics. In our recent work [33] we discuss these algorithms in comparison to our newly developed hierarchical and adaptive algorithm, which we will be employing in this study. The new algorithm reproduces identical trajectories as conventional Metropolis simulations. Originally, the method was optimized for the simulation of the LRIM with nonconserved order parameter and single spin flips. The necessary adaptation for the simulation of the LRIM with conserved order parameter and nearest-neighbor exchanges can be encoded into the set of couplings which is used for the simulation, without any need of further adjustments [34]. The algorithm is characterized by a reduced computational complexity and small prefactors which together lead to massive speedup factors ranging from ≈ 150 for $\sigma = 0.6$ to ≈ 450 for $\sigma = 1.5$ compared with a direct summation of all interactions, for the simulated systems here with $N = L^2 = 1024^2$ spins. For technical details, see the Supplemental Material [34]. Another approach is the use of hardware accelerators. In Ref. [38] an efficient implementation on GPUs was proposed which we expect to yield a speedup of < 20 for our application [39].

Even though the order parameter remains constant, the system becomes more ordered, which is reflected in an increase of the characteristic length $\ell(t)$ with time t. The characteristic length is of interest in two ways: For one

thing, it is needed to check for dynamical scaling, the foundation of the theory of phase-ordering kinetics [4–6]. The other important aspect is the scaling behavior of $\ell(t)$, which for many models can be described by a power law: $\ell(t) \sim t^{\alpha}$ with the growth exponent α. Based on deterministic continuum models [40,41], there exist predictions for the growth laws for general O(n) models [42–44] with conserved and nonconserved order parameter. In particular, for the LRIM with conserved order parameter dynamics the prediction in the asymptotic limit of large t based on the Cahn-Hilliard [41] approach reads as [42–44]

$$\ell(t) \sim t^{\alpha} = \begin{cases} t^{1/3} & \sigma > 1 \\ (t \ln t)^{1/3} & \sigma = 1 \\ t^{1/(2+\sigma)} & \sigma < 1 \end{cases}, \tag{2}$$

independently of the dimension. For $\sigma > 1$ (the potential decays comparatively rapidly) one recovers the Lifshitz-Slyozov exponent $\alpha = 1/3$ known for short-range interacting models from theory [4,45], simulations [46–53], and experiments [54]. At the crossover point $\sigma = 1$ a multiplicative logarithmic correction to the growth is expected. For $\sigma < 1$ (slower decaying potential) a faster growth is predicted, which can be understood qualitatively by additional pseudoforce contributions leading to an effective drift of the domain walls toward each other [55,56]. In equilibrium for $d = 2$, one observes three regimes [57,58]: For $\sigma \leq d/2 = 1$ the mean-field regime, for $d/2 < \sigma \leq 2 - \eta_{\mathrm{sr}}(d) = 7/4$ the intermediate regime with σ-dependent critical exponents, and for $\sigma > 2 - \eta_{\mathrm{sr}}(d)$ the short-range regime [59].

The correspondence between deterministic continuum models and stochastic lattice models is in general rather good, but there are some exceptions. One example is the nonconserved nearest-neighbor Ising model quenched to zero temperature, where one finds $t^{1/2}$ in contrast to $\ln t$ as obtained in the continuum theory [4]. Recently, such deviations have also emerged in case of long-range interactions: While for quenches of the nonconserved LRIM to finite temperatures the corresponding continuum prediction [42–44] was confirmed [32,56], for quenches to zero temperature a deviation from the prediction was found [56,60,61], leading to a σ-independent growth law with nontrivial exponent. For the one-dimensional conserved LRIM, it was argued in Ref. [56] that the underlying mechanism of domain growth is completely different in deterministic continuum and stochastic discrete models. There, analytical considerations and simulations of a simplified model at low temperatures lead to a σ-independent growth with short-range-like behavior $\sim t^{1/3}$. In this light, it is therefore of particular interest to check the prediction [Eq. (2)] obtained via the deterministic continuum Cahn-Hilliard equation [41] for the two-dimensional conserved LRIM.

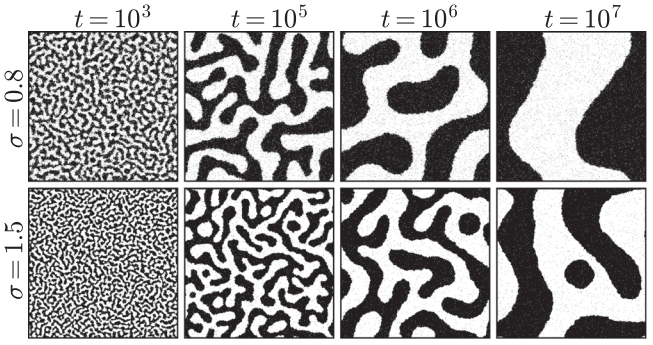

FIG. 1. Snapshots of exemplary time evolutions for $L = 512$, $T = 0.5T_c$. It is very apparent that the phase separation happens faster for $\sigma = 0.8$ (upper row) than for $\sigma = 1.5$ (lower row).

A visual impression of the growing characteristic length $\ell(t)$ during phase separation in a quench to $T = 0.5T_c$ is given in Fig. 1, where one exemplary time evolution is shown for $\sigma = 0.8$ in the upper panels and one for $\sigma = 1.5$ in the lower panels. From these snapshots, it appears that the dynamics is faster for $\sigma = 0.8$ than for $\sigma = 1.5$, which is consistent with the prediction [Eq. (2)], although no statement about prefactors is made there.

For a quantitative investigation, we first check the main feature underlying the kinetics of phase separation [4–6], i.e., dynamical scaling. Dynamical scaling is reflected in the observation that the circular and thermal average of the two-point correlation function

$$C(r,t) = \langle s_i(t) s_j(t) \rangle \tag{3}$$

becomes a function of the scaled distance $r/\ell(t)$ only:

$$C(r,t) = f\left(\frac{r}{\ell(t)}\right), \tag{4}$$

where $r = |\mathbf{r}_{i,j}|$. Dynamical scaling is demonstrated for our simulations in Fig. 2, where we plot $C(r,t)$ versus $r/\ell(t)$ using different times [62] for (a) $\sigma = 0.8$ and (b) $\sigma = 1.5$ with system size $L = 1024$. Here, the characteristic length $\ell(t)$ is self-consistently extracted from the first zero crossing of $C(r,t)$. The quality of the data collapse is excellent, confirming the dynamical scaling hypothesis. The insets show the same data, but unscaled, i.e., $C(r,t)$ versus r. For increasing times, $C(r,t)$ crosses zero at larger distances, reflecting the growing length scale. In both plots, in contrast to the results with nonconserved order parameter [32], an oscillating behavior of the correlation function can be observed. This is in qualitative agreement with the phase separation in the nearest-neighbor model [53].

A related observable is the structure factor $S(\mathbf{k},t) = \int d\mathbf{r} C(\mathbf{r},t) e^{i\mathbf{k}\mathbf{r}}$ defined as the Fourier transform of the correlation function, which is plotted in its scaled form $S(k,t)\ell(t)^{-d}$ vs $k\ell(t)$ in Fig. 3 for (a) $\sigma = 0.8$ and

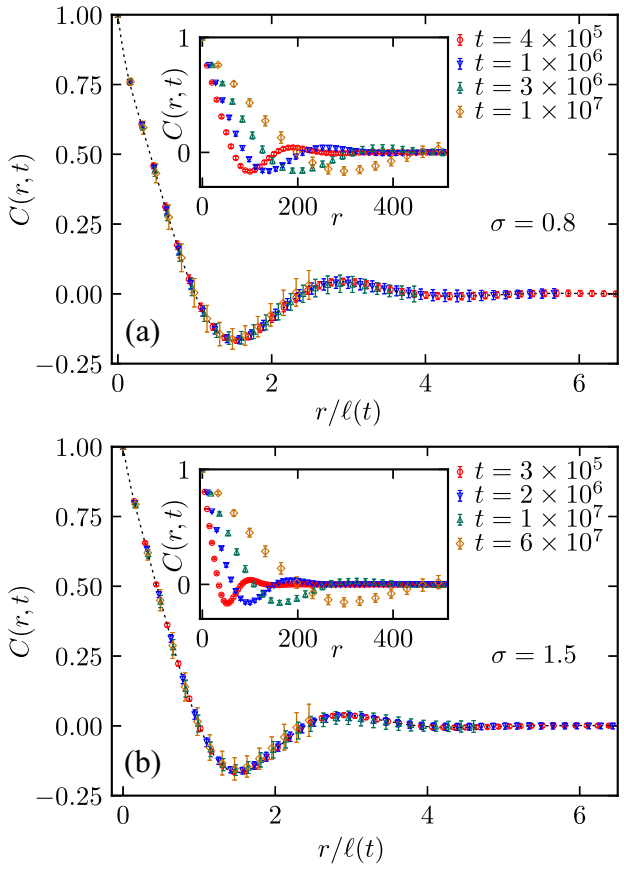

FIG. 2. The correlation function $C(r,t)$ versus the scaled distance $r/\ell(t)$ for system size $L = 1024$ at different times for (a) $\sigma = 0.8$ and (b) $\sigma = 1.5$. The black dotted lines are interpolations which serve as a guide to the eye. In the insets the same data for the unscaled distance are shown.

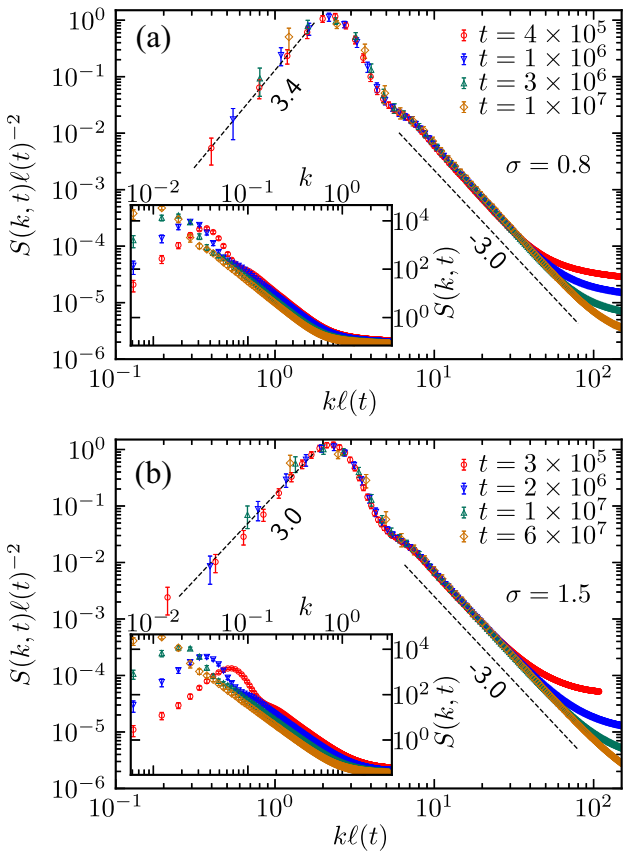

FIG. 3. Scaled structure factor $S(k,t)\ell(t)^{-d}$ versus $k\ell(t)$ for system size $L = 1024$ at different times for (a) $\sigma = 0.8$ and (b) $\sigma = 1.5$. In the insets the same data on unscaled axes are shown.

(b) $\sigma = 1.5$ using the same times and the same definition of $\ell(t)$ as for the correlation function. While in both plots the large k behavior follows Porod's law [63], i.e., $S(k,t) \sim k^{-d-1}$, the small k behavior differs for the two σ. For small k, one expects $S(k,t) \sim k^{\beta}$, where $\beta \geq 4$ from the short-range Cahn-Hilliard equation [64–66]. Our data seem to be best described by effective exponents $\beta \approx 3.4$ for $\sigma = 0.8$ and $\beta \approx 3.0$ for $\sigma = 1.5$, i.e., values that are not compatible with this bound. A precise and safe assessment of β is difficult since the available range of relevant k values is quite small and does not approach sufficiently small k (which are limited by $2\pi/L$). The observed discrepancy from the expected value of $\beta = 4$ is, however, not surprising, since for the nearest-neighbor Ising model even smaller values of $\beta \approx 2.5$ were observed [50].

After the confirmation of the dynamical scaling we now test the deterministic continuum prediction for the LRIM considered here. For this purpose, we plot $\ell(t)$ for different σ on a log-log scale in Fig. 4(a). The solid lines are drawn according to Eq. (2) where the time ranges always start after an initial crossover period and stop at the onset of finite-size effects. For all σ there is a time period over which the data is compatible with the prediction. In the short-range-like regime with $\sigma = 1.5$ and 1.1 the range in which the prediction agrees with the data is substantial. Also for $\sigma = 1$ the observed length scale is very well described by the corresponding functional form in Eq. (2) when admitting an additive logarithmic correction whose strength is determined via an additional constant c leading to $\ell(t) \propto [t \ln(ct)]^{1/3}$. The solid line for $\sigma = 1$ in Fig. 4(a) with $c = 200$ turns out to be quite insensitive to the chosen value of c. In the long-range dominated regime with $\sigma < 1$, the asymptotic regime is still well observable for $\sigma = 0.9$ and 0.8, but the range in which the data follow the prediction becomes shorter. This shows the importance of the large system size $L = 1024$, a fact which is highlighted in the inset of Fig. 4(a). There, for $\sigma = 0.8$ the length scale divided by the predicted growth law $\ell(t)/t^{\alpha}$ for different lattice sizes L is shown. A flat region in this plot corresponds to a time period where the measured growth matches the prediction. For the lattice sizes $L = 256$ and 512 there is no region where the data show a plateau, meaning that only for $L \geq 1024$ the asymptotic behavior can be observed. For $\sigma = 0.6$ the situation becomes even more difficult. It is apparent from Fig. 4(a) that the region

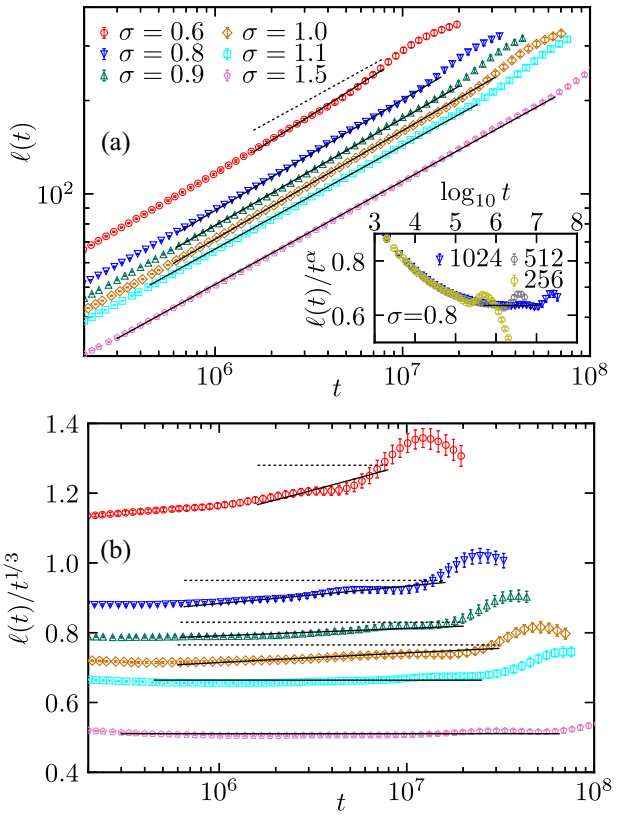

FIG. 4. (a) Characteristic length $\ell(t)$ versus time t for $\sigma = 0.6$, 0.8, 0.9, 1.0, 1.1, and 1.5 and lattice size $L = 1024$ on a log-log scale. The solid lines show the prediction [Eq. (2)]. The dashed line corresponding to $t^{1/3}$ highlights the deviation between short- and long-range growth. In the inset we show the data for $\sigma = 0.8$ divided by the expected growth $t^{\alpha} = t^{1/2.8}$ for three different system sizes. The horizontal black line is drawn over the same t range as the solid line in the main plot. (b) Same data as in (a) but divided by $t^{1/3}$ highlighting the deviation from the short-range growth behavior, represented by the horizontal dashed lines.

compatible with the prediction is relatively short, which can be attributed to even stronger finite-size effects than for the previous two σ values. To emphasize the deviation from the short-range-like growth, we show in Fig. 4(b) the same data and solid lines as in (a) but divided by $t^{1/3}$. For $\sigma \leq 1$, the data are well compatible with the solid lines showing the predicted asymptotic growth law and clearly incompatible with the horizontal dashed lines corresponding to a $t^{1/3}$ behavior. With our data, we can thus rule out a hypothetical short-range-like growth as obtained for the one-dimensional LRIM model for all $\sigma > 0$ in Ref. [56].

Thus the confirmation of the prediction in Eq. (2) required the simulation of a system with more than a million spins (and thereby more than 10^{11} interactions) for more than 10^7 sweeps, enabled by our new algorithm [33]. Simulations with conserved dynamics are in general significantly more difficult than simulations with nonconserved order parameter since the crossover to the asymptotic growth law happens at very late times. This fact cannot be compensated for by the drastic speedup of rejection-free algorithms [50,56] because the low temperatures needed for those approaches to work efficiently shift the crossover to the asymptotic regime to even later times [50]. Furthermore, the simplifications made in Ref. [56] for the one-dimensional model cannot be carried over to higher dimensions, and therefore cannot be applied here. With our new algorithm we are not restricted to low temperatures anymore and do not need any simplifications of the model. Nonetheless the investigation of the phase-separation process remained a big challenge, since for $L = 1024$ the simulation for each of the 1200 realizations (200 for each σ) took more than half a year of wall-clock time to complete. This corresponds to a total CPU time of more than 600 core years with the new algorithm and would have involved more than 100000 core years with a direct summation of the interactions using the same resources. To dispel any last doubts about the growth exponent for $\sigma = 0.6$, where the observation period of the asymptotic behavior is rather short, one would need to simulate $L = 2048$, which is at the verge of feasibility even with our new algorithm.

To conclude, we have for the first time observed the asymptotic scaling prediction in Eq. (2) for the growth of the characteristic length $\ell(t)$ during phase separation in the two-dimensional LRIM with conserved order parameter. Key to this finding was our newly developed algorithm [33] which allows for a very efficient simulation of the LRIM in a nonequilibrium setting. As outlined above, Corberi *et al.* [56] recently found that Eq. (2) does not properly describe the growth of $\ell(t)$ in the one-dimensional case. They argued on general grounds that the good correspondence between noiseless continuum approaches and the discrete Ising model in the nonconserved case does not hold for conserved dynamics because in the latter setting the dynamics in the lattice model is intrinsically stochastic and hence may not be captured by a deterministic continuum theory [56]. In light of their finding for the one-dimensional system, the speculation emerges that the predictions obtained from noiseless continuum approaches may in general not transfer to the discrete Ising model with conserved order parameter. Our observation that $\ell(t)$ does match the prediction for the two-dimensional LRIM thus rules out the hypothesis of a *general* breakdown of this correspondence.

A future perspective is the investigation of the early time behavior during the phase separation of the LRIM at low temperatures, as performed, e.g., in Ref. [56], or the study of phase separation during quenches to the critical temperature [67]. Another possible extension is the investigation of two-time quantities with a focus on aging [67] for which no analytical predictions exist. As recently observed for the nonconserved model in Ref. [68], we expect to find a nontrivial aging exponent.

We thank Suman Majumder for useful discussion. This project was funded by the Deutsche Forschungsgemeinschaft (DFG, German Research Foundation) under Project No. 189853844—SFB/TRR 102 (Project B04), and the Deutsch-Französische Hochschule (DFH-UFA) through the Doctoral College "$\mathbb{L}^4$" under Grant No. CDFA-02-07. We further acknowledge support by the Leipzig Graduate School of Natural Sciences "BuildMoNa."

*fabio.mueller@itp.uni-leipzig.de
†henrik.christiansen@itp.uni-leipzig.de
‡Present address: NEC Laboratories Europe GmbH, Kurfürsten-Anlage 36, 69115 Heidelberg, Germany.
‖wolfhard.janke@itp.uni-leipzig.de

[1] P. Chomaz, M. Colonna, and J. Randrup, Nuclear spinodal fragmentation, Phys. Rep. **389**, 263 (2004).
[2] A. A. Hyman, C. A. Weber, and F. Jülicher, Liquid-liquid phase separation in biology, Annu. Rev. Cell Dev. Biol. **30**, 39 (2014).
[3] R. Shimizu and H. Tanaka, A novel coarsening mechanism of droplets in immiscible fluid mixtures, Nat. Commun. **6**, 1 (2015).
[4] A. J. Bray, Theory of phase-ordering kinetics, Adv. Phys. **51**, 481 (2002).
[5] *Kinetics of Phase Transitions*, edited by S. Puri and V. Wadhawan (CRC Press, Boca Raton, 2009).
[6] R. Livi and P. Politi, *Nonequilibrium Statistical Physics: A Modern Perspective* (Cambridge University Press, Cambridge, England, 2017).
[7] J. K. Hoffer and D. N. Sinha, Dynamics of binary phase separation in liquid ^{3}He-^{4}He mixtures, Phys. Rev. A **33**, 1918 (1986).
[8] P. Ao and S. Chui, Two stages in the evolution of binary alkali Bose-Einstein condensate mixtures towards phase segregation, J. Phys. B **33**, 535 (2000).
[9] J. Hofmann, S. S. Natu, and S. Das Sarma, Coarsening Dynamics of Binary Bose Condensates, Phys. Rev. Lett. **113**, 095702 (2014).
[10] J. Fan, T. Han, and M. Haataja, Hydrodynamic effects on spinodal decomposition kinetics in planar lipid bilayer membranes, J. Chem. Phys. **133**, 235101 (2010).
[11] M. C. Marchetti, J.-F. Joanny, S. Ramaswamy, T. B. Liverpool, J. Prost, M. Rao, and R. A. Simha, Hydrodynamics of soft active matter, Rev. Mod. Phys. **85**, 1143 (2013).
[12] S. Alberti, Phase separation in biology, Curr. Biol. **27**, R1097 (2017).
[13] S. Jiang, J. B. Fagman, C. Chen, S. Alberti, and B. Liu, Protein phase separation and its role in tumorigenesis, eLife **9**, e60264 (2020).
[14] T. Yoshizawa, R.-S. Nozawa, T. Z. Jia, T. Saio, and E. Mori, Biological phase separation: Cell biology meets biophysics, Biophys. Rev. Lett. **12**, 519 (2020).
[15] D. Boyanovsky, H. De Vega, and D. Schwarz, Phase transitions in the early and present universe, Annu. Rev. Nucl. Part. Sci. **56**, 441 (2006).
[16] J. Binney and S. Tremaine, *Galactic Dynamics* (Princeton University Press, Princeton, NJ, 2011).
[17] G. L. Eyink and K. R. Sreenivasan, Onsager and the theory of hydrodynamic turbulence, Rev. Mod. Phys. **78**, 87 (2006).
[18] R. H. French, V. A. Parsegian, R. Podgornik, R. F. Rajter, A. Jagota, J. Luo, D. Asthagiri, M. K. Chaudhury, Y. M. Chiang, S. Granick *et al.*, Long range interactions in nanoscale science, Rev. Mod. Phys. **82**, 1887 (2010).
[19] Y. Levin, R. Pakter, F. B. Rizzato, T. N. Teles, and F. P. C. Benetti, Nonequilibrium statistical mechanics of systems with long-range interactions, Phys. Rep. **535**, 1 (2014).
[20] A. Campa, T. Dauxois, D. Fanelli, and S. Ruffo, *Physics of Long-Range Interacting Systems* (Oxford Scholarship, Oxford, 2014).
[21] J. S. Douglas, H. Habibian, C.-L. Hung, A. V. Gorshkov, H. J. Kimble, and D. E. Chang, Quantum many-body models with cold atoms coupled to photonic crystals, Nat. Photonics **9**, 326 (2015).
[22] B. Neyenhuis, J. Zhang, P. W. Hess, J. Smith, A. C. Lee, P. Richerme, Z. Gong, A. V. Gorshkov, and C. Monroe, Observation of prethermalization in long-range interacting spin chains, Sci. Adv. **3**, e1700672 (2017).
[23] Y.-C. Zhang, V. Walther, and T. Pohl, Long-Range Interactions and Symmetry Breaking in Quantum Gases Through Optical Feedback, Phys. Rev. Lett. **121**, 073604 (2018).
[24] M. K. Hazra and Y. Levy, Biophysics of phase separation of disordered proteins is governed by balance between short- and long-range interactions, J. Phys. Chem. B **125**, 2202 (2021).
[25] K. Kawasaki, Diffusion constants near the critical point for time-dependent Ising models. I, Phys. Rev. **145**, 224 (1966).
[26] E. Luijten and H. W. J. Blöte, Monte Carlo method for spin models with long-range interactions, Int. J. Mod. Phys. C **06**, 359 (1995).
[27] K. Fukui and S. Todo, Order-N cluster Monte Carlo method for spin systems with long-range interactions, J. Comput. Phys. **228**, 2629 (2009).
[28] E. Flores-Sola, M. Weigel, R. Kenna, and B. Berche, Cluster Monte Carlo and dynamical scaling for long-range interactions, Eur. Phys. J. Special Topics **226**, 581 (2017).
[29] M. Michel, X. Tan, and Y. Deng, Clock Monte Carlo methods, Phys. Rev. E **99**, 010105(R) (2019).
[30] J. Barnes and P. Hut, A hierarchical $O(N \log N)$ force-calculation algorithm, Nature (London) **324**, 446 (1986).
[31] J. W. Perram, H. G. Petersen, and S. W. De Leeuw, An algorithm for the simulation of condensed matter which grows as the $3/2$ power of the number of particles, Mol. Phys. **65**, 875 (1988).
[32] H. Christiansen, S. Majumder, and W. Janke, Phase ordering kinetics of the long-range Ising model, Phys. Rev. E **99**, 011301(R) (2019).
[33] F. Müller, H. Christiansen, S. Schnabel, and W. Janke, Fast, hierarchical, and adaptive algorithm for Metropolis Monte Carlo simulations of long-range interacting systems, arXiv:2207.14670.
[34] See Supplemental Material at http://link.aps.org/supplemental/10.1103/PhysRevLett.129.240601 which includes additional Refs. [35–37]. The Supplemental Material contains an introduction to the methods used.

[35] P. Ewald, Die Berechnung optischer und elektrostatischer Gitterpotentiale, Ann. Phys. (Berlin) **369**, 253 (1921).
[36] M. E. J. Newman and G. T. Barkema, *Monte Carlo Methods in Statistical Physics* (Oxford University Press, New York, 1999).
[37] S. Schnabel and W. Janke, Accelerating polymer simulation by means of tree data-structures and a parsimonious Metropolis algorithm, Comput. Phys. Commun. **256**, 107414 (2020).
[38] Y. Liang, X. Xing, and Y. Li, A GPU-based large-scale Monte Carlo simulation method for systems with long-range interactions, J. Comput. Phys. **338**, 252 (2017).
[39] The authors of Ref. [38] reported a speedup of ≈440 in a very dilute setting. In our study we work in the completely different regime of a very dense system where a pre-rejection scheme (which is highly non-trivial in a parallel implementation) is crucial for a good performance. See Supplemental Material [34] for a more detailed discussion.
[40] V. L. Ginzburg and L. D. Landau, On the theory of superconductivity, Zh. Eksp. Teor. Fiz. **20**, 1064 (1950).
[41] J. W. Cahn and J. E. Hilliard, Free energy of a nonuniform system. I. Interfacial free energy, J. Chem. Phys. **28**, 258 (1958).
[42] A. J. Bray, Domain-growth scaling in systems with long-range interactions, Phys. Rev. E **47**, 3191 (1993).
[43] A. J. Bray and A. D. Rutenberg, Growth laws for phase ordering, Phys. Rev. E **49**, R27 (1994).
[44] A. D. Rutenberg and A. J. Bray, Energy-scaling approach to phase-ordering growth laws, Phys. Rev. E **51**, 5499 (1995).
[45] I. M. Lifshitz and V. V. Slyozov, The kinetics of precipitation from supersaturated solid solutions, J. Phys. Chem. Solids **19**, 35 (1961).
[46] D. A. Huse, Corrections to late-stage behavior in spinodal decomposition: Lifshitz-Slyozov scaling and Monte Carlo simulations, Phys. Rev. B **34**, 7845 (1986).
[47] J. G. Amar, F. E. Sullivan, and R. D. Mountain, Monte Carlo study of growth in the two-dimensional spin-exchange kinetic Ising model, Phys. Rev. B **37**, 196 (1988).
[48] C. Roland and M. Grant, Monte Carlo Renormalization-Group Study of the Late-Stage Dynamics of Spinodal Decomposition, Phys. Rev. Lett. **60**, 2657 (1988).
[49] G. Barkema, J. Marko, and J. De Boer, Transient and asymptotic domain growth in the 3D Ising model with conserved spin, Europhys. Lett. **26**, 653 (1994).
[50] J. F. Marko and G. T. Barkema, Phase ordering in the Ising model with conserved spin, Phys. Rev. E **52**, 2522 (1995).
[51] D. W. Heermann, L. Yixue, and K. Binder, Scaling solutions and finite-size effects in the Lifshitz-Slyozov theory, Physica (Amsterdam) **230A**, 132 (1996).
[52] S. van Gemmert, G. T. Barkema, and S. Puri, Phase separation driven by surface diffusion: A Monte Carlo study, Phys. Rev. E **72**, 046131 (2005).
[53] S. Majumder and S. K. Das, Domain coarsening in two dimensions: Conserved dynamics and finite-size scaling, Phys. Rev. E **81**, 050102(R) (2010).
[54] B. D. Gaulin, S. Spooner, and Y. Morii, Kinetics of Phase Separation in $Mn_{0.67}Cu_{0.33}$, Phys. Rev. Lett. **59**, 668 (1987).
[55] B. P. Lee and J. L. Cardy, Phase ordering in one-dimensional systems with long-range interactions, Phys. Rev. E **48**, 2452 (1993).
[56] F. Corberi, E. Lippiello, and P. Politi, One dimensional phase-ordering in the Ising model with space decaying interactions, J. Stat. Phys. **176**, 510 (2019).
[57] J. Sak, Recursion relations and fixed points for ferromagnets with long-range interactions, Phys. Rev. B **8**, 281 (1973).
[58] T. Horita, H. Suwa, and S. Todo, Upper and lower critical decay exponents of Ising ferromagnets with long-range interaction, Phys. Rev. E **95**, 012143 (2017).
[59] Note, that for $\sigma = 1$, $d = 2$ plays the role of an upper critical dimension, where also logarithmic corrections appear.
[60] R. Agrawal, F. Corberi, E. Lippiello, P. Politi, and S. Puri, Kinetics of the two-dimensional long-range Ising model at low temperatures, Phys. Rev. E **103**, 012108 (2021).
[61] H. Christiansen, S. Majumder, and W. Janke, Zero-temperature coarsening in the two-dimensional long-range Ising model, Phys. Rev. E **103**, 052122 (2021).
[62] The times for which the dynamical scaling is probed are chosen such that they cover the asymptotic growth law regime and are hence different for $\sigma = 0.8$ and $\sigma = 1.5$.
[63] G. Porod, General theory, in *Small Angle X-ray Scattering*, edited by O. Glatter and O. Kratky (Academic Press, London, 1982), p. 17.
[64] C. Yeung, Scaling and the Small-Wave-Vector Limit of the Form Factor in Phase-Ordering Dynamics, Phys. Rev. Lett. **61**, 1135 (1988).
[65] H. Furukawa, Comment on "Scaling and the Small–Wave-Vector Limit of the Form Factor in Phase-Ordering Dynamics", Phys. Rev. Lett. **62**, 2567 (1989).
[66] H. Furukawa, Multi-time scaling for phase separation, J. Phys. Soc. Jpn. **58**, 216 (1989).
[67] F. Müller, H. Christiansen, and W. Janke (to be published).
[68] H. Christiansen, S. Majumder, M. Henkel, and W. Janke, Aging in the Long-Range Ising Model, Phys. Rev. Lett. **125**, 180601 (2020).